International Journal of Heat and Mass Transfer 52 (2009) 3799–3804

Contents lists available at ScienceDirect

International Journal of Heat and Mass Transfer

journal homepage: www.elsevier.com/locate/ijhmt

Characteristics of direct-contact, skin-surface temperature sensors

S.K.S. Boetcher [a], E.M. Sparrow [b,*], M.V. Dugay [a]

[a] Department of Mechanical and Energy Engineering, Center for Advanced Scientific Computing and Modeling (CASCaM), University of North Texas, Denton, TX 76207-7102, USA
[b] Laboratory for Heat Transfer and Fluid Flow Practice, Department of Mechanical Engineering, University of Minnesota, Minneapolis, MN 55455-0111, USA

ARTICLE INFO

Article history:
Received 5 January 2009
Received in revised form 10 February 2009
Accepted 10 February 2009
Available online 23 April 2009

Keywords:
Skin temperature
Temperature sensor
Biomedical
Bioheat
Human healthcare

ABSTRACT

Numerical simulations have been performed to determine the performance characteristics of direct-contact devices for the measurement of skin-surface temperature. Such devices consist of a thin metallic foil which serves as a heat spreader backed by a foam insulation pad. The sensor, either a miniature thermocouple or thermistor, is adhered to the heat-spreading foil. In practice, such devices operate in the transient mode, and the numerical simulations were performed in that mode. Special focus was given to three relevant parameters which contribute significantly to the accuracy of the temperature measurements: (a) the thickness of the foam pad, (b) the thermal conductivity of the pad material, and (c) the contact resistance between the device and the skin surface. It was found that the presence of the foam pad significantly degraded the accuracy of the measured temperature. Diminishing the thickness or, in the limit, elimination of the pad is believed necessary to enable the device to provide temperatures of acceptable accuracy. An alternative and suitable approach to the achievement of satisfactory accuracy is to use pad materials of higher thermal conductivity than those presently being utilized. With regard to contact resistance, the presence of an air gap between the device and the skin surface of the thickness of a sheet of paper did not cause a significant error in the temperature indicated by the device.

1. Introduction

A knowledge of the skin-surface temperature is useful as a diagnostic tool in the assessment of human health. There are a number of commercially available devices for the accomplishment of this temperature measurement, with the direct-contact type being most favored by clinicians. These devices usually include a miniature thermocouple or thermistor as the sensing element. The sensing element is threaded into a layered assembly which, in one manifestation, consists of a thin metal foil backed by a layer of compliant foam. The thin metal foil serves as a heat spreader. An adhesive is applied to the skin-facing side of the foil. In another manifestation, the metal foil is replaced by a plastic strip that is coated with adhesive on both of its faces. Such devices are commercially available under brand names such as Mono-a-therm (Nellcor, Pleasanton, CA successor to Mallinckrodt Medical, St. Louis, MO) and Vital Sense (Bend, OR).

It is relevant to assess the accuracy of the temperature measured by such devices. There are two factors which immediately suggest themselves as possible causes of error: (a) the insulating nature of the foam backing pad and (b) the thermal contact resistance at the interface between the heat spreader and the skin surface. Both of these factors serve to impede the heat flow from the skin surface to the ambient. It is expected that the presence of such impedances would give rise to a temperature elevation of the skin beneath the measurement device. In fact, the recognition that the blockage of the skin-surface heat flow elevates the skin-surface temperature has been used as the basis of a device to measure deep-tissue temperature [1–8].

In view of the issues raised in the preceding paragraph, it is remarkable that an in-depth investigation of the potential errors inherent in direct-contact, foam-backed temperature sensors appears not to have been published. The only somewhat relevant work is confined to experimental comparisons of direct-contact devices with other modalities of skin temperature measurement, without discussion of the insulating role of the foam [9–11].

The work reported here is an in-depth numerical simulation of the performance of direct-contact, skin-surface temperature-measuring devices. The simulations encompass the heat transfers in the tissue layers beneath the measuring device, the heat transfers within the device proper, and the convective-radiative heat transfers from the exposed surfaces to the environment. All direct-contact devices which measure human body temperatures necessarily operate in the transient mode. Consequently, the numerical simulations performed here are necessarily of a transient nature. The specific foci of the present investigation are the assessment of the impacts of the characteristics of the foam pad (its thickness and thermal conductivity) and the thermal contact resistance at the device–skin interface on the accuracy of the temperature measurement.

* Corresponding author. Tel.: +1 612 625 5502; fax: +1 612 625 5230.
E-mail address: esparrow@umn.edu (E.M. Sparrow).

0017-9310/$ - see front matter © 2009 Elsevier Ltd. All rights reserved.
doi:10.1016/j.ijheatmasstransfer.2009.02.011

Nomenclature

c	specific heat [J/kg °C]
h	heat transfer coefficient [W/m^2 °C]
k	thermal conductivity [W/m °C]
L	thickness [mm]
T	temperature [°C]
t	time [s]
R_i	device radius [mm]
R_o	solution domain radius [mm]
r, z	cylindrical coordinates [mm]
ρ	density [kg/m^3]
ω	blood perfusion [(m^3/s)/m^3]

Subscripts

a	arterial
b	blood
c	copper
f	fat layer
g	air gap
i	material identification index
m	muscle layer
p	foam-backing pad
rad	radiation
s	skin layer
∞	ambient

2. Description of the physical and mathematical model

It is convenient to refer to Fig. 1 to aid in the description of the physical model. A tissue bed consisting of parallel layers of skin, fat, and muscle separates the exposed surface from the body core which has a fixed temperature of 37 °C. The temperature-sensing device is shown atop the skin surface. As previously indicated, it consists of a heat spreader and a foam backing pad. For this analysis, the heat spreader will be taken as a thin copper foil. Not shown in the figure is the temperature sensor proper. Its miniature size is sufficiently small so that its presence can be neglected without loss of accuracy. The model conveyed in Fig. 1 is based on an axisymmetric temperature-measuring device. The device radius is R_i. The solution domain defined by the radius R_o is taken sufficiently large so that for radial positions that extend beyond R_o, there is no effect of the presence of the sensing device. Heat transfer by combined convection and radiation occurs at the exposed surfaces of the sensing device and of the skin.

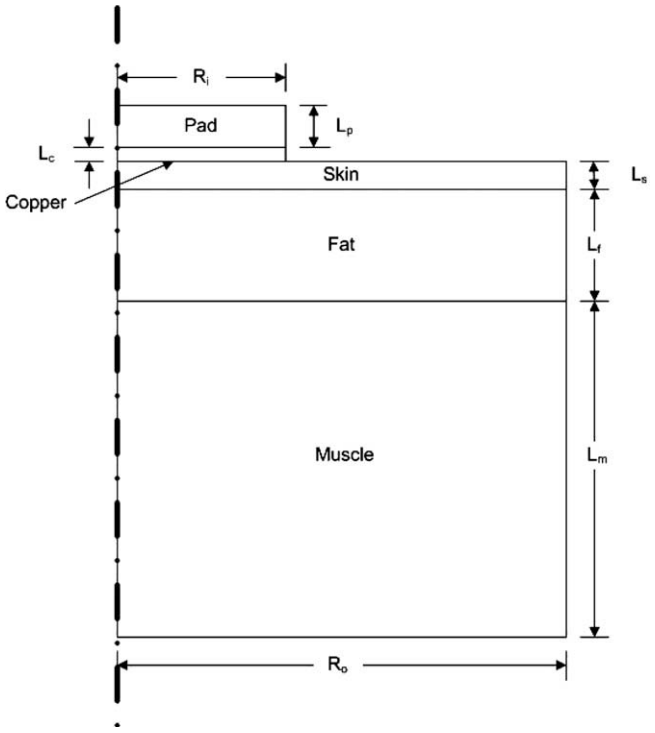

Fig. 1. Schematic diagram of an axisymmetric view of the foam pad and copper heat spreader situated atop a section of skin, fat, and muscle.

The solution domain consists of five individual materials. For each of these layers, the transient heat conduction is governed by the First Law of Thermodynamics. Those layers which represent tissue include, in addition to heat transfer by conduction, a pseudo-convective transfer which is termed *perfusion*. When perfusion is included, it is common to refer to that form of the First Law as the bio-heat equation. The bio-heat equation, expressed in a form applicable to any one of the tissue layers, is

$$(\rho c)\frac{\partial T_i}{\partial t} = k_i\left[\frac{1}{r}\frac{\partial}{\partial r}\left(r\frac{\partial T_i}{\partial r}\right)+\frac{\partial^2 T_i}{\partial z^2}\right] + \omega_{b,i}\rho_b c_b(T_i - T_a) \tag{1}$$

In this equation, the subscript i respectively pertains to the skin layer (s), to the fat layer (f), and to the muscle layer (m). Therefore, Eq. (1) represents three equations. The equation includes the specific material properties of each layer, ρ, c, and k, the blood-flow perfusion rate ω, the blood properties ρ_b and c_b, and the temperature of the artery blood T_a which feeds the tissue bed. The artery blood temperature is assumed to be equal to the temperature of the body core (37 °C). The blood perfusion rate ω may be different in each of the tissue layers.

The bio-heat equation as stated in Eq. (1) is due to Pennes [12]. There have been many critiques of the logic underlying the Pennes equation, e.g., [13]. Notwithstanding those critiques, the Pennes bio-heat equation is the overwhelming choice of investigators of thermal processes in the human body.

The other two material layers, the copper heat spreader and the foam backing pad, obey the traditional heat equation, which is given by

$$(\rho c)_i\frac{\partial T_i}{\partial t} = k_i\left[\frac{1}{r}\frac{\partial}{\partial r}\left(r\frac{\partial T_i}{\partial r}\right)+\frac{\partial^2 T_i}{\partial z^2}\right] \tag{2}$$

Here, the subscript i refers to either the copper heat spreader (c) and the backing pad (p). As noted earlier, the analysis will also consider a thermal contact resistance at the interface of the temperature-measuring device and the skin surface. The model used for the contact resistance is an air gap of height L_g. The governing equation for heat conduction through the air gap is also represented by Eq. (2) in which the subscript i is replaced by g.

All told, the solution of the problem involves simultaneous treatment of five (or six, in the case of contact resistance) partial differential equations which depends on two space coordinates and time. Clearly, a numerical solution method is mandatory. For this purpose, ANSYS thermal software was employed. That software makes use of finite elements. For the present problem, meshes consisting of 150,000 and 300,000 nodes were employed. The use of the two different numbers of nodes was based on the need to demonstrate mesh independence. That independence

was demonstrated by a survey of the temperature results which showed an accuracy of approximately 0.02%. Subsequent to the demonstration, the main body of results was obtained using the 150,000-mesh discretization.

To complete the statement of the problem, it is necessary to specify the initial condition, the boundary conditions, and the conditions of continuity at the interfaces between the layers. At the interface between the muscle layer and the body core, the temperature was specified as 37 °C. At all other layer-layer interfaces, temperature and heat flux continuity was required. At the exposed surfaces of the measurement device and the skin, account was taken of heat transfer by radiation and convection. With regard to the former, the radiative transfer was linearized so that a radiation heat transfer coefficient h_{rad} was obtained. This linearization enabled the radiative and convective heat transfer coefficients to be added so that both processes could be represented by a single heat transfer coefficient h that was prescribed. At the outer boundary of the solution domain, $r = R_o$, it was assumed that the presence of the device was not felt, so that an adiabatic boundary condition was applied.

The values of the material properties and the dimensions of the model are presented in Table 1. The heat transfer coefficient h was chosen to be 13.6 W/m^2 °C, which corresponds to black radiative surroundings and minimal room ventilation. For the ambient temperature, a value of 22 °C was imposed.

A number of parameters were varied during the course of the investigation. The thickness of the foam backing pad was assigned values of 3.048, 1.524, and 0 mm. In addition, the conductivity of the foam was varied from 0 to 0.06 W/m °C. The blood perfusion was also parametrically varied between a value of 0 and 0.005 s^{-1}.

To obtain a proper initial condition for the transient studies, auxiliary data runs were made for steady-state conditions in which the temperature-sensing device was absent from the skin surface. The steady-state temperature distribution that was obtained in this way was used as the initial condition for the transient simulations.

3. Results and discussion

3.1. Effect of thickness of foam backing pad

The first issue to be addressed is the impact of the thickness of the foam backing pad on the accuracy of the temperature measured by a sensor situated at the interface of the copper heat spreader and the skin surface. The results which display the effect of different thicknesses of the pad are conveyed in Figs. 2–4, respectively for foam thermal conductivities of 0 (a limiting case), 0.03, and 0.06 W/m °C. In each figure, the sensor temperature is plotted as a function of time for each of the three investigated foam thicknesses. Also appearing in each figure is the actual surface temperature which would occur in the absence of the temperature-measuring device. For the conditions of these results, it was found that the temperature of a centrally positioned sensor was essentially identical to a sensor situated beneath the outer edge of the measuring device.

Table 1
Dimensions and material properties.

	L_i [mm]	k [W/m °C]	ρ [kg/m^3]	c [J/kg °C]	$\rho_b c_b$ [J/m^3 °C]	ω_b [(m^3/s)/m^3]
Skin	2.03	0.62	1100	3500	4×10^6	0
Fat	8.89	0.48	960	2500		0.003
Muscle	22.9	1.26	1040	3600		0.005
Foam	3.05	0, 0.03, 0.06	24	1130	–	–
Copper	0.30	380.5	8930	385	–	–
Air	0.076	0.0223	1.16	1010	–	–

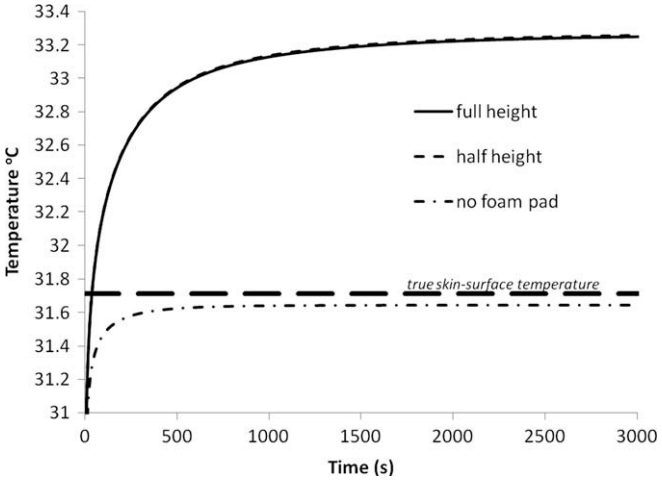

Fig. 2. Skin-surface temperature plotted against time for foam thermal conductivity = 0 W/m °C and for parametric values of the pad thickness.

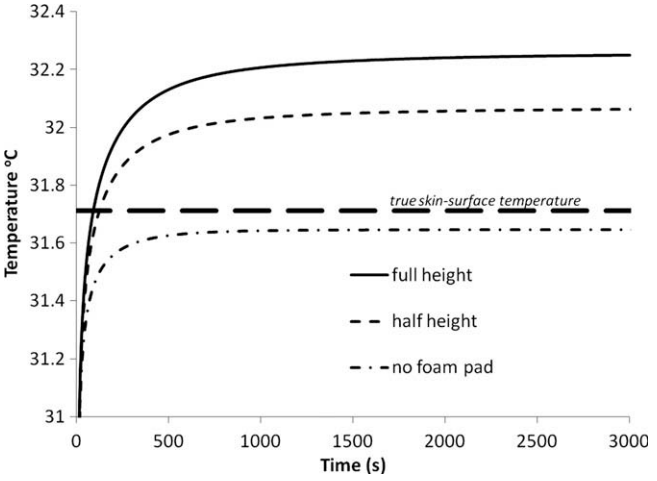

Fig. 3. Skin-surface temperature plotted against time for foam thermal conductivity = 0.03 W/m °C and for parametric values of the pad thickness.

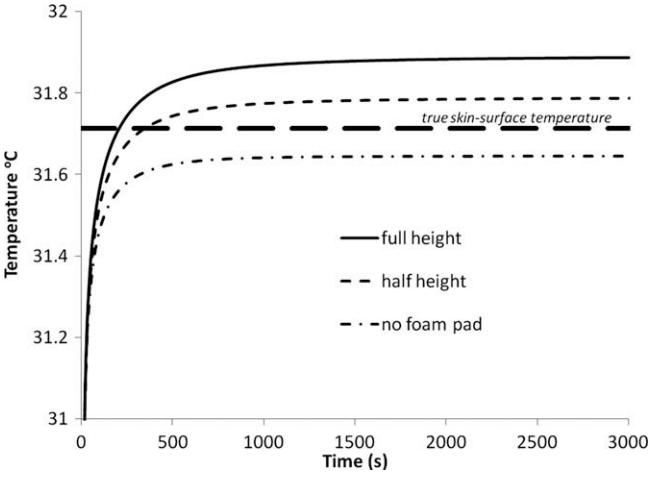

Fig. 4. Skin-surface temperature plotted against time for foam thermal conductivity = 0.06 W/m °C and for parametric values of the pad thickness.

Attention is first turned to Fig. 2. In this case, where the thermal conductivity is zero, the actual thickness of the foam is irrelevant as long as any foam layer is present. This expectation is verified

by the congruity of the full-height and half-height temperature results. Only when the foam is absent is there a major impact of the foam thickness. Noteworthy in the figure is the significant difference in the temperature measured with the foam in place and the true skin temperature. In the absence of the foam, there is a slight difference between the sensor temperature and the true temperature that is due to the presence of the copper heat spreading film. It is, however, interesting to note that the indicated temperature for the no-foam case is actually lower than the true surface temperature. While this finding may appear, at first thought, to be an anomaly, it is readily explainable by physical reasoning. The copper foil is an excellent conductor so that its temperature is uniform throughout. When the foil is in place, it provides an additional exposed surface area beyond that of the skin surface proper. This additional surface area is due to the finite height of the foil. The lower temperature of the sensor situated beneath the foil is due to the foil's enhanced heat transfer capability that results from its finite height.

Focus is next directed to the results corresponding to the foam thermal conductivity of 0.03 W/m °C. This value of conductivity is that of a very good insulator. Inspection of Fig. 3 shows that in the presence of a finite thermal conductivity, the thickness of the foam pad does play a role in contrast to the behavior shown in Fig. 2. In particular, it is seen that the temperature beneath the full-height pad is approximately 0.2 °C higher than that for the half-height foam pad. Furthermore, for the steady state, the presence of the full-height pad creates a temperature error of approximately 0.6 °C relative to the true skin temperature. Once again, there is a small difference between the temperature for the pad-absent case and the true temperature due to the presence of the copper heat spreader.

The next case to be considered is that for which the pad has a thermal conductivity of 0.06 W/m °C. While materials with thermal conductivities of this level may still be regarded as insulators, they would not be considered to be excellent insulators. With the increase of the thermal conductivities characterizing Figs. 3 and 4, it is to be expected that the temperature errors due to the presence of the foam would decrease, and inspection of those figures verifies this expectation. The steady-state error in evidence for the full-height pad has been reduced to 0.25 °C due to the conductivity increase to 0.06 W/m °C.

Figs. 3 and 4 continue to confirm the finding that the temperature sensed centrally beneath the temperature-measuring device is more or less equal to that sensed under the edge of the device, as was already mentioned in connection with Fig. 2. The two main messages of Figs. 2–4 are that more accurate temperature results can be obtained by (a) use of the thinnest possible foam pads and (b) utilization of a foam material whose conductivity is as high as possible.

3.2. Effect of contact resistance

Even for machined surfaces, thermal contact resistance exists. In the present instance, where a thin metallic film is in contact with a flexible medium such as the surface of the skin, thermal contact resistance is inevitable. On the basis of qualitative experiments performed by the authors, it was concluded that a reasonable estimate of the contact resistance could be obtained by envisioning an air gap between the thin metallic film and the skin surface, the thickness of which is on the order of the thickness of a piece of paper (0.076 mm). With the use of this model of the contact resistance, the problem becomes one of solving six simultaneous equations, as was already mentioned. Although it was not strictly necessary, the heat capacity of the air gap was taken into account in addition to its thermal conductivity.

The temperature versus time results that correspond to the presence of the air gap are conveyed in Fig. 5. For this figure, the foam backing pad is of full height and the thermal conductivity of the foam material is 0.03 W/m °C. From the figure, it is seen that the presence of the air gap leads to a slight increase in the temperature of the centrally positioned sensor. The extent of this temperature elevation is about 0.1 °C. From the standpoint of practice, this change of temperature due to the air gap is not significant. It is interesting to note that in the absence of the foam, but with an air gap present, the sensor provided steady-state temperatures that are more or less the same as the true temperature. This outcome reflects an interesting balance between the insulating effect of the air gap and the additional heat loss area provided by the edge of the copper film.

In the absence of the air gap, Figs. 2–4, the temperatures of a centrally positioned sensor and of one positioned beneath the outboard edge of the temperature-measuring device were more or less identical. However, with both the air gap and foam present, this equality of the centrally positioned and edge-positioned sensor temperatures no longer occurs, with the edge-measured temperature being about 0.2 °C lower than that of the centrally measured temperature.

3.3. Steady-state temperature results

The first steady-state result to be presented is focused on defining the role of the magnitude of the blood perfusion, and Fig. 6 has been prepared in this regard. The figure is a plot of the skin-surface temperature as a function of radial position for the full-height foam pad with a thermal conductivity of 0.03 W/m °C. No air gap was considered for this situation. The figure shows that the temperature results are virtually independent of the perfusion rate. The perfusion rates displayed in this figure were chosen to be both less than and greater than the perfusion rate of 0.003 s^{-1} that was used for the remainder of the calculations.

The next issue to be highlighted is the effect of foam height and an air-gap presence/absence on the steady-state temperature distribution along the skin surface. These results are presented in Fig. 7 for a foam conductivity of 0.03 W/m °C and an air-gap thickness of 0.076 mm. The figure contains five curves, respectively for (a) full-height foam, no air gap, (b) full-height foam, air gap, (c) no foam, no air gap, (d) no foam, air gap, and (e) true skin-surface temperature. Although five curves were plotted, only four appear in the figure because the results for cases (d) and (e) coincided precisely. It can be seen from the figure that in the presence of the full-height foam and the air gap there is a temperature variation along

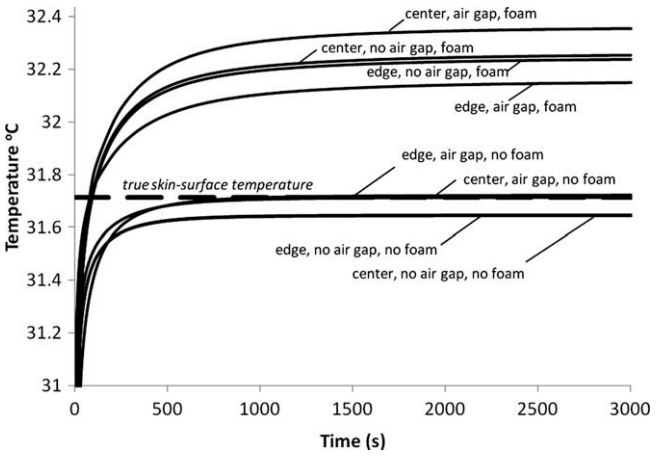

Fig. 5. Comparison of skin-surface temperatures with and without the air gap for foam thermal conductivity = 0.03 W/m °C and for a full-height foam pad.

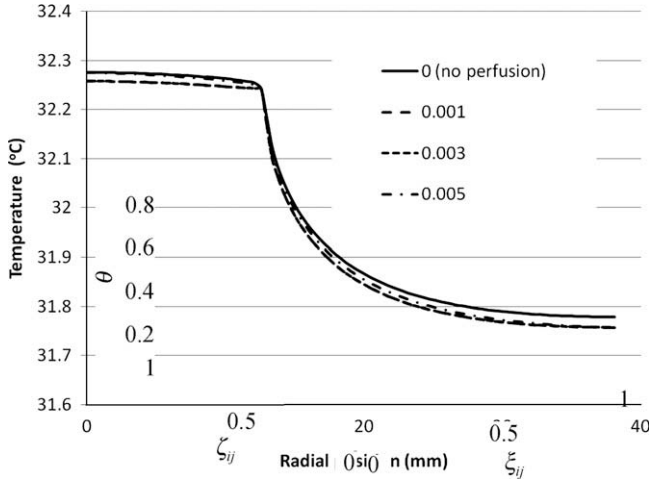

Fig. 6. Steady-state skin-surface temperature plotted as a function of radial distance for several values of blood perfusion for $k = 0.03$ W/m °C.

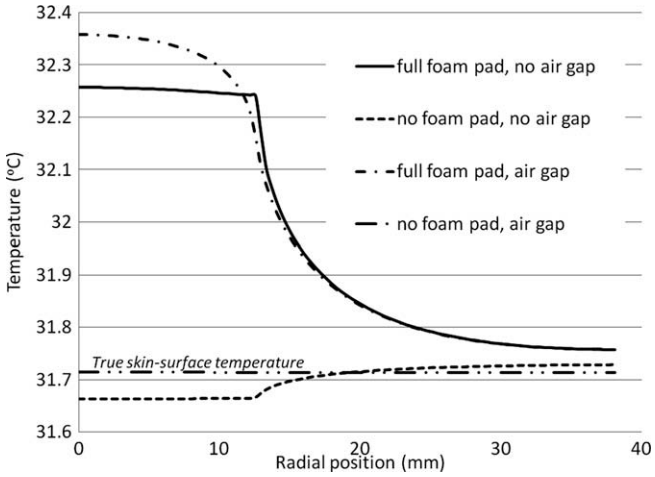

Fig. 7. Steady-state skin-surface temperature plotted as a function of radial distance for several foam-pad and air-gap arrangements for $k = 0.03$ W/m °C.

that part of the skin surface that lies beneath the temperature-measuring device. On the other hand, in the absence of the air gap and with the full-height foam, the variation of the temperature under the air gap is on the order of 0.01 °C. Also noteworthy is that with the full height of the foam present, the temperature difference between the sensor and the true skin-surface temperature is significant from the standpoint of practice, being on the order of 0.5–0.6 °C. For the cases in which the foam pad is absent, the temperature variation along the surface is either exactly zero or insignificant. As explained earlier, the under-device temperatures for the no-foam, no-air-gap case are slightly lower than the true temperature.

The final information to be conveyed are contour diagrams showing the steady-state temperature field. Figs. 8(a–c) present these diagrams respectively for full-height, half-height, and no-height foam pads for a pad thermal conductivity of 0.03 W/m °C and no air gap. In viewing these figures, it is appropriate to focus on the departures of the isotherms from the horizontal. The isotherms themselves are defined as the boundaries between adjacent blocks. In Fig. 8(a), the most noteworthy feature is an S-shaped isotherm just beneath the surface of the skin. Since the lines of heat flow are perpendicular to an isotherm, it is clear that the heat flow is responding to the blockage imposed by the temperature-sensing device by following a path which leads it away from the blockage. At deeper distances beneath the skin, the isotherms become horizontal, reflecting the fact that the presence of the blockage has a finite-depth impact. For the case of the half-height pad, Fig. 8(b), the tendency of the heat to flow away from the blockage continues in force while the removal of the pad, Fig. 8(c), leads to near-surface isotherms that are virtually horizontal. Closer inspection of Fig. 8(c) reveals a tendency for heat to flow toward the site of the copper foil. This effect has been explained earlier.

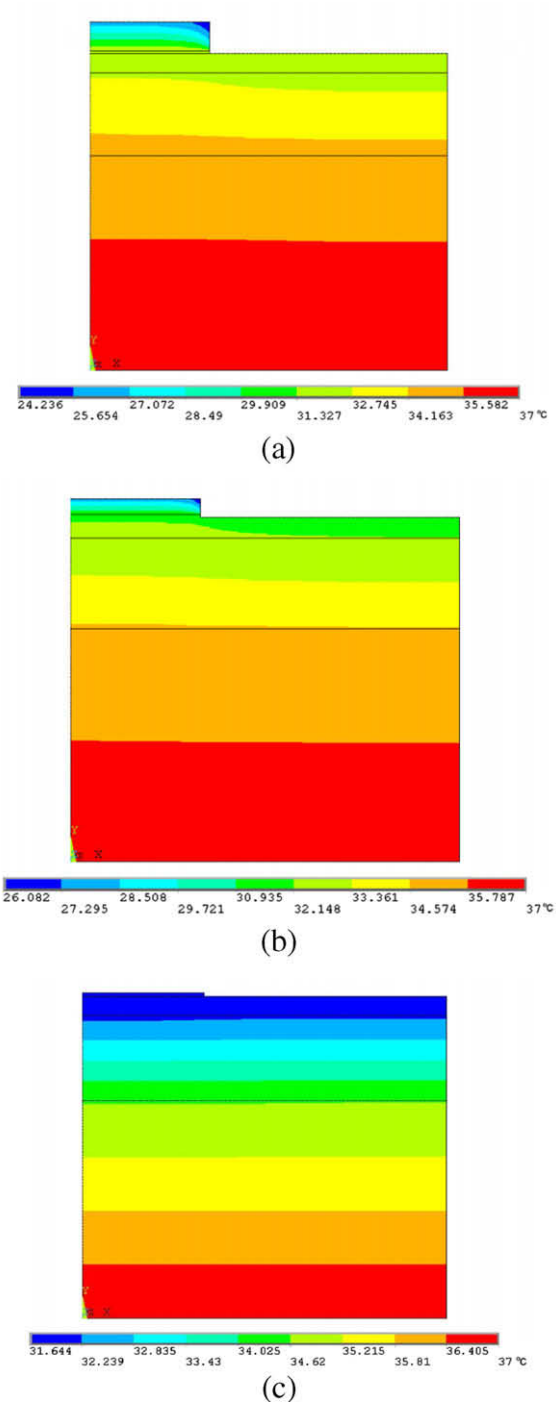

Fig. 8. Steady-state temperature contour diagrams for (a) full-height foam, (b) half-height foam, and (c) no foam for $k = 0.03$ W/m °C.

4. Concluding remarks

The numerical simulations performed here provide strong evidence that the presence of a foam backing pad as a component

of the direct-contact temperature-sensing device is a clear cause of measurement error. It is, therefore, relevant to inquire about why such pads are in common use. It is believed that the reasoning used to support the use of the pads is to "protect the measuring device from being overly influenced by the ambient conditions." The spurious nature of this reasoning can be demonstrated by the recognition that the ambient conditions are equally imposed on the exposed surface of the skin as well as on the exposed surface of the measurement device. It is a fact that the true skin-surface temperature is affected by ambient conditions.

The practical conclusions that can be drawn from the present study are: (a) a foam pad of minimum thickness should be used (if such a pad is deemed necessary), (b) the material of the pad should be chosen to have as high a thermal conductivity as possible consistent with the other functions of the pad, and (c) contact resistance in the form of an air gap of paper thickness does not significantly influence the measured temperature.

References

[1] R.H. Fox, A.J. Solman, A new technique for monitoring the deep body temperature in man from the intact skin surface, J. Physiol. 212 (1971) 8P–10P.
[2] R.H. Fox, A.J. Solman, R. Isaacs, A.J. Fry, I.C. McDonald, A new method for monitoring deep body temperatures from the skin surface, Clin. Sci. 44 (1973) 81–86.
[3] T. Kobayashi, T. Nemoto, A. Kamiya, T. Togawa, Improvement of deep body thermometer for man, Ann. Biomed. Eng. 3 (1975) 181–188.
[4] R.H. Fox, A.J. Solman, Temperature measurement, United States Patent 3 (1976).
[5] S. Muravchick, Deep body thermometry during general anesthesia, Anesthesia 58 (1983) 271–275.
[6] T. Matsukawa, D.I. Sessler, M. Ozaki, K. Hanagata, H. Iwashita, T. Kumazawa, Comparison of distal oesophageal temperature with 'deep' and traceal temperatures, Can. J. Anesth. 44 (1997) 433–438.
[7] M. Yamakage, A. Namiki, Cellular mechanisms of airway smooth muscle relaxant effects of anesthetic agents, J. Anesth. 17 (2003) 251–258.
[8] D. Brajkovic, M.B. Ducharme, Confounding factors in the use of the zero-heat-flow method for non-invasive muscle temperature measurement, Eur. J. Appl. Physiol. 94 (2005) 386–391.
[9] P.C. Szlyk, I.V. Sils, J.D. Ferguson, W.T. Matthew, R.W. Hubbard, Evaluation of insulated miniature thermistors for skin temperature measurement in the rat, Army Research Institute of Environmental, Medicine, Natick, MA, 1986. August.
[10] B.F. Krause, Accuracy and response time comparisons of four skin temperature-monitoring devices, Nurse Anesth. 4 (1993) 55–61.
[11] R.S. Burnham, R.S. McKinley, D.D. Vincent, Three types of skin-surface thermometers: a comparison of reliability, validity, and responsiveness, Am. J. Phys. Med. Rehabil. 85 (2006) 553–558.
[12] H.H. Pennes, Analysis of tissue and arterial blood temperatures in the resting human forearm, J. Appl. Physiol. 1 (1948) 93–122.
[13] E.H. Wissler, Pennes' 1948 paper revisited, J. Appl. Physiol. 85 (1998) 31–41.